Fluid inclusion study of tin-mineralized greisens and quartz veins in the Penouta apogranite (Orense, Spain)*

J. MANGAS

Department of Geology, Faculty of Marine Sciences, University of Las Palmas de Gran Canaria, Campus de Tafira, 35017 Las Palmas de Gran Canaria (Spain)

AND

A. ARRIBAS

Directorate-General XII, Science, Research and Development, Commission of the European Communities, Rue de la Loi 200, B-1049 Brussels, Belgium

Abstract

The Penouta deposit is associated with a small Hercynian apogranite stock that intrudes Precambrian–Cambrian gneisses of the Ollo de Sapo Formation. Tin ore occurs as disseminations of cassiterite in the apogranite and as greisenized zones and quartz veins which traverse both the alkaline leucogranite and the surrounding metamorphic country rocks.

A fluid-inclusion study, utilizing microthermometric, crushing tests and Raman spectroscopic techniques on quartz from an intragranitic vein and a greisen of the host rock, indicates that the evolution of fluids was similar in both samples and occurred in the three main stages: The first stage is characterized by complex CO_2 (CO_2–N_2–CH_4–H_2S) and complex CO_2 aqueous (H_2O–NaCl–CO_2–N_2–CH_4–H_2S) fluids of low salinity (T_m ice > -6 °C), homogenization temperatures between 250 and 410 °C, homogenization pressures below 900 bars, and thermobarometric trapping conditions with temperatures below 700 °C and pressures below 3250 bars. These fluids were probably responsible for the greisenization of the apogranite and wall rocks, and the precipitation of cassiterite. The second stage is represented by low-salinity aqueous solutions (H_2O–NaCl) with T_m ice ≥ -4.5 °C, trapped at homogenization temperatures between 110 and 300 °C and homogenization pressures below 100 bars. This stage can be correlated with kaolinization. The third stage is characterized by higher salinity aqueous fluids (T_m ice ≥ -16.5 °C) containing Na^+ and other cations, trapped at homogenization temperatures between 100 and 130 °C and homogenization pressures below 5 bars. These fluids can be associated with the epigenetic or supergene phases of the orebody.

KEYWORDS: fluid inclusions, thermobarometry, apogranite, greisen, quartz veins, cassiterite.

Introduction

THE Sn–W metallogenic province of the Iberian Peninsula is one of the most important in the Hercynian orogenic belt of Europe. The deposits extend from Galicia through the north of Portugal to the southwest of Spain. They are located exclusively in the Hesperic Massif and a large number of them are in the Central Iberian Zone. The predominant Central Iberian Zone rocks consist of Hercynian granites and a monotonous, late Precambrian–Cambrian, flyschoid marine sequence 'Schist–Greywacke Complex', Ordovician and Silurian rocks are also present. Although there are stratabound deposits, some of which related to volcanism, the most important deposits are related to the syn- to late-tectonic Hercynian granites. The latter include the following types: disseminated cassiterite in apogranite, stanniferous pegmatites and quartz veins with cassiterite, wolframite and scheelite.

Cassiterite, less commonly columbite and tantalite are disseminated in the apical parts of many

* This paper was presented at the ECROFI X Conference. See the following two papers and the Mineralogical Magazine for June 1990.

Mineralogical Magazine, June 1991, Vol. 55, pp. 211–223

tin-albitized granites, which represent the final stages of the magmatic evolution. The granites often show intense and complex post-magmatic alteration, with albitization, muscovitization, greisenization and kaolinization developing on a large and small scale. The emplacement of these apogranites is generally conditioned by regional tectonics, and thus they usually appear as dykes with varying morphology or small intrusive stocks. Frequently associated with these orebodies are tin pegmatites and peribatholith vein deposits.

Typical disseminated tin orebodies include Penouta and Laza (Orense), Golpejas (Salamanca), Torrecilla de los Angeles (Trasquilón) and Portezuelo-Cañaveral (Cáceres). Their paragenesis generally consists of quartz, albite, potash feldspar, muscovite, cassiterite, columbite, tantalite, tapiolite, ilmenite, rutile, apatite and, occasionally gold and fluorite (Arribas, 1979).

Despite the economic importance of these deposits, there have been very few fluid-inclusion studies; only Golpejas has received detailed investigation (Mangas, 1981; Mangas and Arribas, 1984). This paper presents the physico–chemical characteristics of the fluids which gave rise to the mineralization and to the alteration found in the Penouta orebody, using microthermometric, crushing test and Raman spectrometric analyses.

Regional geology

The Penouta tin deposit is located in the eastern part of Orense province (Spain) and 1.5 km from Penouta (Fig. 1). From the geotectonic point of view, the orebody is located in the extreme west of the West-Asturian zone, since it is found within the antiform in whose core the porphyroids of Ollo de Sapo outcrop.

The oldest rocks in the area are the Viana Series and overlying Ollo de Sapo Formation; both of Upper Precambrian or Lower Cambrian age. The Viana Series consists of gneisses, mica schists, quartzites, amphibolites and calcsilicate rocks which originally corresponded to pelitic sandy platform sediments of variable depth. The Ollo de Sapo Formation is composed of porphyritic gneisses with large potash feldspar crystals found within schist matrix containing quartz, feldspar and mica. The structure of the anticline of Ollo de Sapo extends from the north coast of Galicia, disappearing below the Tertiary of the Duero River Basin in the province of Zamora, and continuing on through the Central Belt. Its origin is still under discussion, though these rocks seem to be volcano-sedimentary in nature (Capote, 1983).

The most important igneous rocks comprise an Upper Ordovician–Silurian orthogneiss, the albite granite of Penouta and the late granodiorites; the latter related to the Hercynian orogeny.

After the emplacement of the youngest granitoids, a series of strike-slip faults with N–S and N 40°E strike were formed which displace all earlier structures.

Penouta deposit

The Penouta deposit is associated with a small Hercynian apogranite stock that intrudes Precambrian–Cambrian gneisses of the Ollo de Sapo Formation (Fig. 2A). The apogranite is discordant to the host rocks, since the foliation of the apogranite does not coincide with the schistosity of the wall rocks. Tin ore occurs as disseminations of cassiterite in the apogranite and as greisenized zones and quartz veins which traverse both the alkaline leucogranite and adjoining metamorphic rocks (Fig. 2A,B, Fig. 3).

The leucogranite shows quartz, albite, microcline and muscovite as essential minerals with cassiterite, tantalite, zircon and garnet as accessory minerals. The quartz forms sub-circular porphyroblasts with annular alignments of small plagioclase inclusions. The plagioclase is albite (4% anorthite), and together with microcline and muscovite, shows a flow texture (Fig. 2C,D). The microcline occurs as large crystals with albite inclusions and rims of later albite (Fig. 2C). At times, this feldspar is completely kaolinized. Small cassiterite crystals, ranging in size from 0.03 to 0.04 mm are distributed among and within the muscovite and feldspar (Fig. 2D).

Greisenization of the granite cupola extends outwards along fractures into the country rocks (Fig. 2A and Fig. 3). During this process, quartz, muscovite and cassiterite formed; the cassiterite crystals measuring 0.05 to 0.5 mm. Later, the Penouta granite gave rise to a swarm of N–S trending quartz veins of variable dip. The margins of these veins are characterized by muscovite, feldspar and large cassiterite crystals with tapiolite inclusions (Fig. 3). During the final phase of alteration, the leucogranite and its host rocks were kaolinized.

The main economic interest of the deposit is represented by the disseminated Sn–Ta mineralization which diminishes laterally and in depth. The greisenized zones and veins are relatively unimportant. Kaolin constitutes a minor mineral resource.

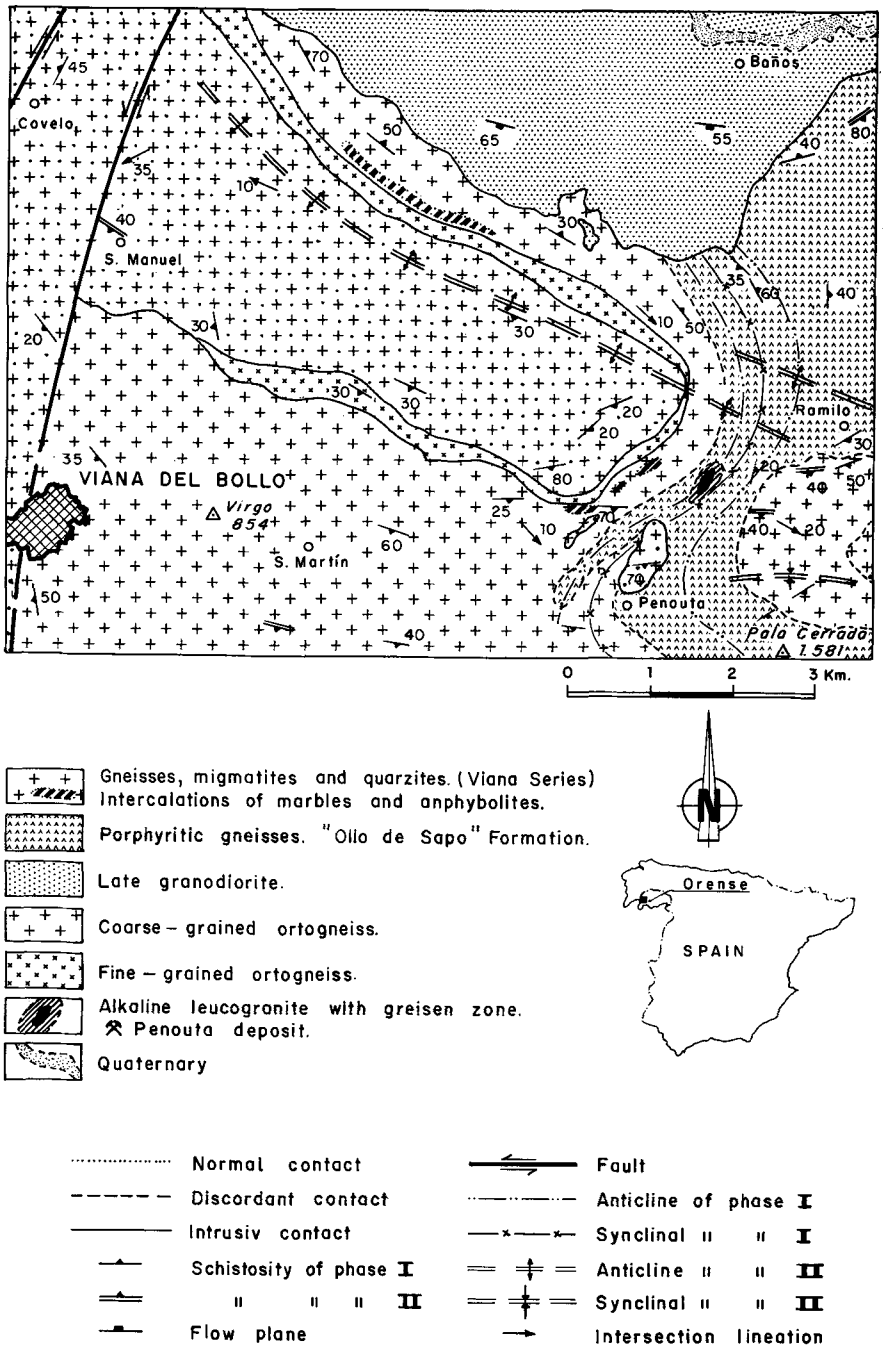

FIG. 1. Geological map of the Viana del Bollo zone showing location of the Penouta orebody (adapted from Iglesias and Varea, 1981).

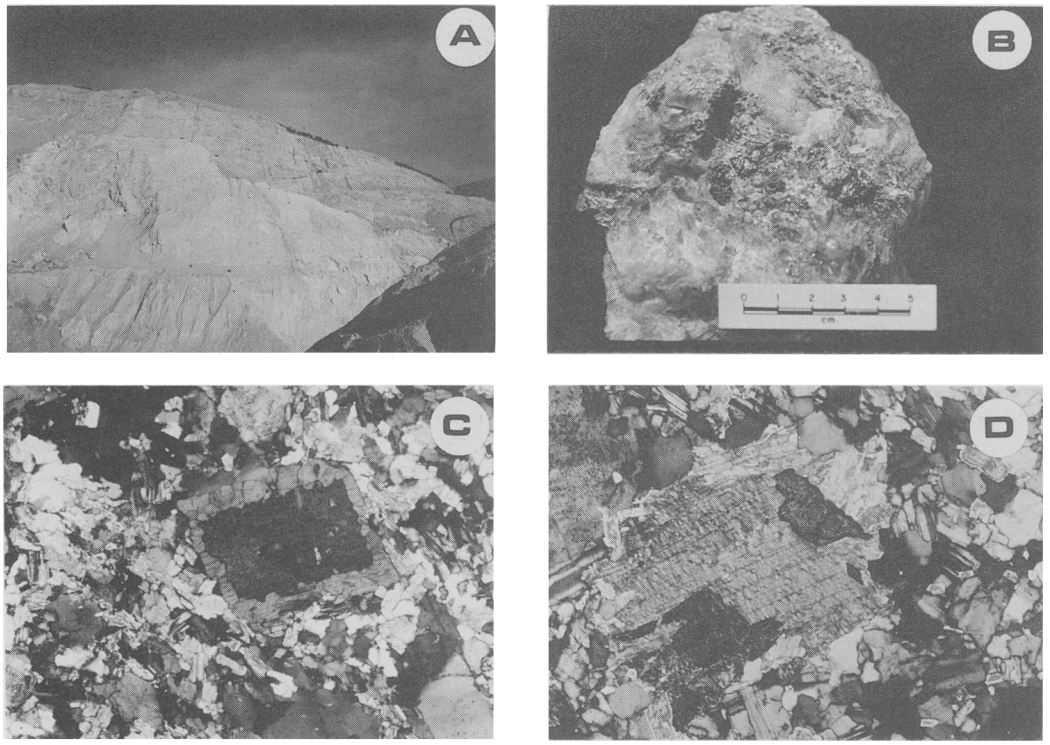

FIG. 2. A, Penouta open-pit. Intrusive contact between Penouta apogranite and Ollo de Sapo Formation gneisses. B, sample of mineralized quartz vein. Cassiterite is found towards the edges of the vein together with muscovite and quartz. C, Thin section of the Penouta albitic granite (×25 Crossed Nicols). Microcline rimmed by albite is observed in centre of photograph. D, Thin section ×63 (Crossed Nicols). Cassiterite appears disseminated in the apogranite, here next to muscovite.

From the petrological standpoint, the Penouta deposit shows three principal stages: magmatic, hydrothermal (greisen and quartz veins) and supergene, and corresponds to the so-called 'alkaline microgranites with columbite and tantalite' mineralizations (Arribas, 1979). At present, the orebody is not mined.

Fluid inclusions

Description of inclusions. The fluid inclusion study was undertaken using microthermometry, crushing tests and Raman spectroscopy. Three samples were analysed: an intragranitic vein (P34), a greisen (P115) and an exogranitic vein (P42), (Fig. 3).

Microthermometric studies of fluid inclusions were performed on 300 μm-thick plates using a microscope equipped with a UMK50 Leitz objective and a Chaixmeca cooling and heating stage (Poty *et al.*, 1976). Crushing test analysis was carried out on a crushing stage designed by the Department of Geology at the University of Salamanca (Spain). Raman spectrometric measurements were made at room temperature using a M.O.L.E.-type microprobe at CREGU, Nancy (France) (Dhamelincourt *et al.*, 1979). The exciting radiation was the 514.5 nm green line from a 5-W Spectra Physics ionized argon laser. The photomultiplier was an RCA 31034 type cooled to −20 °C. The presence of CO_2, CH_4, N_2 and H_2S in the gas part of the inclusions was checked using a 1–W laser beam, referring to the following lines, respectively: 1388 cm^{-1}, 2915 cm^{-1}, 2331 cm^{-1}, and 2611 cm^{-1}.

Observations show that the quartz is crossed by a large number of microfractures of varying strike, dip and extension, representing repeated fracturing, healing and recrystallization. Different quartz grains with distinctive shapes and orientation are seen. In the grains, the inclusions are generally pseudosecondary or secondary in character (Roedder, 1984). In addition, a smaller number of inclusions appear isolated or in groups; these are interpreted as

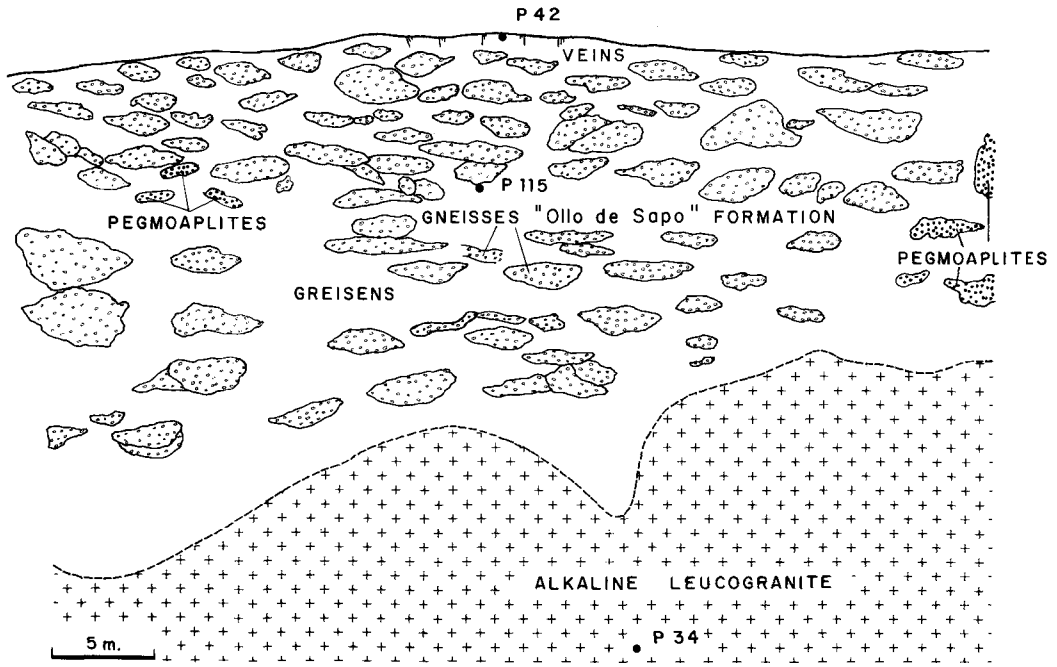

FIG. 3. Scheme of Fig. 2A, where the location of samples taken for fluid inclusion study is shown.

primary (Roedder, 1984). The abundance of fluid inclusions and mineral impurities is highly variable giving rise to transparent, translucent and opaque areas in the quartz. Inclusion morphology is equally varied, ranging from 5 to 50 μm in size.

Based on the estimated composition of the trapped fluid using microthermometric, crushing test and Raman data, and the volume of the fluid phases at room temperature, four types of inclusions have been defined (Fig. 4A, B, C and D):

Type 1: complex, CO_2 aqueous inclusions (H_2O–NaCl–CO_2–N_2–CH_4–H_2S). These show two (mainly H_2O L + CO_2 V) or three phases (mainly H_2O L + CO_2 L + CO_2 V) at room temperature ($T \approx 20$ °C). The carbon-rich phases (CO_2 L + CO_2 V) occupy ≥20% of the total volume of inclusions. The volumetric proportion of CO_2 L relative to CO_2 L + CO_2 V (Flc) is ≥30%. These inclusions which are the most representative of the Penouta orebody, appear in all the samples and are found distributed in microfractures, isolated, or in groups (Fig. 4A and B).

Type 2: complex, CO_2 inclusions (CO_2–N_2–CH_4–H_2S). These inclusions are one (CO_2 L/CO_2 V) or two phases (mainly CO_2 L + Co_2 V) at room temperature and the Flc data are ≥30%. These inclusions are rare in samples P34 and P42, and are not seen in sample P115. They appear near groups and fractures containing type 1 inclusions (Fig. 4B).

Type 3: low salinity, aqueous inclusions (H_2O.–NaCl). These show one (H_2O L) or two phases (H_2O L + H_2O V) at room temperature in which the vapour bubble occupies 2 to 20% of the total inclusion volume. These inclusions appear in all the samples and are fracture controlled (Fig. 4C).

Type 4: mixed salt, aqueous inclusions (H_2O–NaCl and other salts). These show one (H_2O L) or two (H_2O L + H_2O V) at room temperature in which the vapour bubble occupies ≤5% of the total inclusion volume. These inclusions are comparatively scarce and are always secondary in character (Fig. 4D).

Microthermometric results

More than 200 fluid inclusions have been studied in samples P34 and P115. The microthermometric results are summarized in Table 1 and described below.

Melting temperatures for solid CO_2 in type 1 nd 2 inclusions, and clathrate melting temperatures for type 1 inclusions show that the carbonic phase contains CO_2 and other gases (Swanenberg, 1979). Fluid salinities estimated from final ice

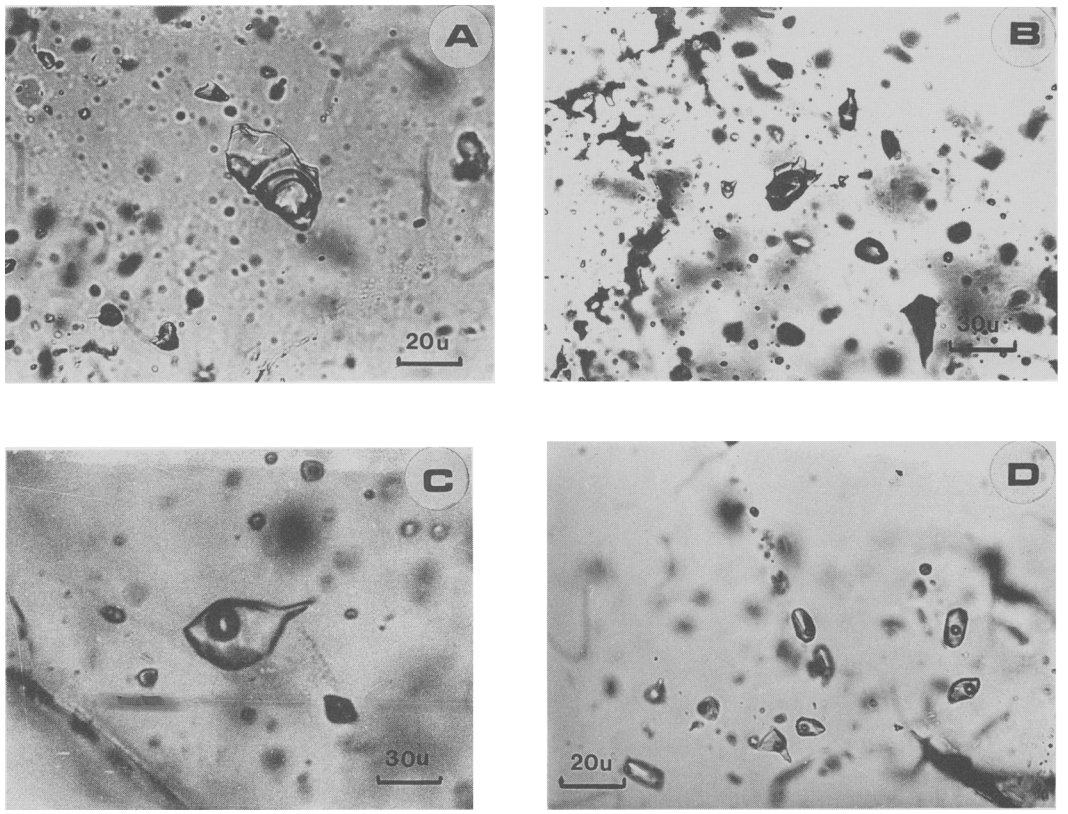

FIG. 4. A, A three-phase fluid inclusion in the centre of photo, containing mainly liquid H_2O, liquid CO_2 and gaseous CO_2. B, Distributions of groups of type 1 and 2 inclusions. C, Type 3 aqueous inclusion containing water and water vapour. D, Distribution of type 4 aqueous inclusions in healed fracture planes.

TABLE 1. Microthermometric results, Penouta deposit. No = total number of inclusions studied; T_m CO_2 = temperature of final melting of CO_2 solid (°C); T_m clat. = clathrate melting temperature (°C); T_h CO_2 = temperature of homogenization of CO_2 liquid and vapour phases (°C); T_h = temperature of total homogenization (°C); G and L = homogenization into gaseous and liquid states, respectively. Salinity, expressed in terms of weight per cent NaCl equivalent. The maximum frequency in the results is underlined.

SAMPLES	Type of inclusion	No	Tm_{CO_2}	Tm_{ice}	Tm_{clat}	Salinity	Th_{CO_2} and Type of homogenization	Th and type of homogenization
P 34	1	35	-56.6/-58.5 -57.3	-2/-6 -4.5	8/15 9.5	<8.5 7.1	17/27 L and G 23.5 L and25.5 G	260/410 L and G 325 L and 385 G
Intragranitic vein	2	12	-57/-59 -57.5	--	--	--	17/26 L and G 22 L and G	--
	3	47	--	0.5/-4.5 -3.3	--	1.5/7 6.3	--	110/300 L 165 L
	4	9	--	-15.5/-16.5 -16	--	> 19 19.6	--	115/130 L 120 L
P 115	1	40	-57/-59 -58	-2.5/-5 -3.3	9.5/11 10.5	< 7 5.4	16/21 L and G 19.5 L and G	250/320 L 285 L
Greisen	3	68	--	0/-4 -2.7	--	0/6 4.8	--	110/280 L 185 L
	4	6	--	-9.5/-11.5 -10.5	--	>13.7 14.5	--	100/120 L 115 L

melting temperatures (T_m ice) in type 3 inclusions (Potter *et al.*, 1978) and final clathrate melting temperature (T_m clat) in type 1 inclusions (Collins, 1979) are low (≥8.5 wt.% eq. NaCl). In the type 4 inclusion the initiation of ice melting varied between −22 and −50 °C, and thus indicates the presence of not only Na^+ but minor amounts of other cations (Crawford *et al.*, 1979). Salinity estimates, based on T_m ice values for the system NaCl–H_2O (Potter *et al.*, 1978), range between 13.5 and 19 wt.% eq. NaCl.

Homogenization temperatures for the non-aqueous part of type 1 and 2 inclusions indicate variable densities between 0.15 and 0.85 g/cm^3 (Angus *et al.*, 1976). However, using the diagrams of Swanenberg (1979), it is deduced that the $X(CH_4)$ in the CO_2 phase is lower than 0.1 for T_m CO_2 > −59 °C and for Flc data >30%. In the same way, the density of the non-aqueous part of type 1 and 2 inclusions that homogenize into the gas and liquid state ranges between 0.25 and 0.75 g/cm^3. Temperatures of total homogenization for all inclusion types vary between 100 and 410 °C. Type 1 inclusions homogenize into the liquid and gaseous state high temperatures (250–410 °C) whereas type 3 and 4 inclusions homogenize into the liquid state at lower temperatures (100–300 °C).

Some type 1 and 2 inclusions decrepitated at temperatures between 200 and 300 °C, before total homogenization. With reference to the *T*-salinity graph of Bodnar (1983), the density of the Penouta type 1 inclusions varies between 0.5 and 0.85 g/cm^3, type 3 inclusions between 0.8 and 1 g/cm^3 and type 4 inclusions beween 1 and 1.1 g/cm^3.

The microthermometric results described above suggest that the fluid inclusions trapped in quartz samples P34 and P115 are evidence of continuous hydrothermal evolution. At an early stage, circulation and trapping of carbonic and low salinity, carbonic–aqueous fluids containing N_2, CH_4 and H_2S, took place. This was followed by progressively more aqueous fluids and a steady decrease in volatile content. Thus, in sample P34 (intragranitic vein) there is a transition between complex CO_2 aqueous inclusions which homogenize into the gaseous state at temperatures ranging between 340 and 410 °C and those which homogenize into the liquid state between 260 and 340 °C. Subsequently, weakly saline aqueous solutions containing less than 7 wt.% eq. NaCl appeared with homogenization temperatures from 300 to 100 °C. However, below 180 °C, very dilute aqueous fluids with salinities between 0 and 4 wt.% eq. NaCl were also trapped. During the final stages of fluid evolution, more saline solutions were present (13.5 and 19 wt.% eq. NaCl). These contained various cations and were trapped at temperatures of approximately 100 °C in the quartz.

Results of the crushing test

Crushing of quartz grains from the edge and core of the veins was carried out in anhydrous glycerine, about five tests being performed on each sample. The observations reveal the constant presence of CO_2 fluids. In accordance with the classification proposed by Leroy (1978), the liberated gas intensity in all the tests reaches high to very high values (Fig. 5). Sample P34 shows low to very high releases, due to the quartz having clear and transparent areas, where the number of inclusions is low compared to the translucent areas.

Raman spectroscopic analyses

Raman spectroscopic analyses have been made for seven inclusions characteristic of the deposit: five type 1 inclusions (sample P34, fluid inclusions nos. 2, 41 and 42; sample P115, fluid inclusions nos. 13 and 33), one type 2 (sample P34, fluid inclusion no. 19), nd one type 3 (sample P34, fluid inclusion no. 9). The physical and microthermometric properties of these inclusions are shown in Table 2. The analyses were carried out solely on the vapour phase part of the type 1 and 2 inclusions. Calculation of the molar fractions (Table 3) indicates the presence of significant CO_2 with minor N_2, CH_4 and H_2S.

From the Raman and microthermometric results, bulk composition, densities and isochores were calculated for each of the inclusions using the program of Debussy and Ramboz [CREGU and CRPG, Nancy, France] (Ramboz *et al.*, 1985). These are summarized in Table 3. The results show that for samples P34, the type 1 inclusions though having different homogenization temperatures, and homogenizing into different states, have a similar global composition. Moreover, there are no significant differences in the global composition of the type 1 inclusions from the intragranitic vein (P34) and the greisen quartz (P115). The ratio $H_2O > CO_2 > NaCl > N_2 \geq CH_4$ is seen throughout.

Type 2 inclusions have the composition $CO_2 > N_2 > CH_4 > H_2S$. By comparison, the type 3 inclusions are predominantly aqueous and contain no detectable volatiles in the vapour phase.

TABLE 2. Physical characteristics of the fluid inclusions analysed by Raman microprobe and corresponding microthermometric data. Abbreviations as for Table 1. No. = reference number of fluid inclusion; % vol. = volume per cent of liquid (L) and vapour (G) phases, at room temperature ($T \approx 20$ °C).

CHARACTERISTICS						MICROTHERMOMETRIC DATA				
SAMPLES	Nº F.I.	Type	Phases	% Vol	Size (μm)	Tm_{CO_2}	Tm_{ice}	Tm_{clat}	Th_{CO_2}	Th
P34	2	1	H_2O L CO_2 G	85 15	20	-58.2	-3	9.6	22 G	308 L
P34	41	1	H_2O L CO_2 G	60 40	10	-57.7	-3.2	9.6	--	382 G
P34	42	1	H_2O L CO_2 G	60 40	20	-57	-4.5	9.5	25.3 L	328 L
P115	13	1	H_2O L CO_2 G	60 40	20	-58.2	-4.4	10.6	18.9 G	288 L
P115	33	1	H_2O L CO_2 G	70 30	15	-58.2	-3.2	11.2	18.8 G	282 L
P34	19	2	CO_2	--	15	-57.8	--	--	19.1 L	--
P34	9	3	H_2O L H_2O G	95 5	10	--	-1.9	--	--	244 L

Thermobarometric trapping conditions and discussion

The trapping conditions of the inclusions studied by Raman microprobe were estimated using the experimental data for H_2O (Fisher, 1976), CO_2 (Bergman, 1982) and H_2O–CO_2–NaCl (Gehrig, 1980), since there are no data for the real system H_2O–NaCl–CO_2–N_2–CH_4–H_2S. The volatile content of type 1 and 2 inclusions was simplified assuming $X_{CO_2} = X_{CO_2} + X_{N_2} + X_{CH_4} + X_{H_2S}$. In the *P–T* diagram of Fig. 6, the isochores for the inclusions were projected onto the equilibrium curves for the compositions calculated by Raman microprobe.

The minimum thermobarometric conditions for the complex CO_2 aqueous inclusions (nos. 2, 41 and 42 in the intragranitic vein and nos. 13 and 33 in the greisen) correspond to 300–380 °C and 300–1000 bars.

In sample P34, since the type 1 and 2 inclusions appear primary and decrepitate in the same temperature interval (between 200 and 300 °C) they are assumed to be contemporaneous. Therefore, as a first approximation, the intersection of the isochores for those type 1 and 2 inclusions which homogenize into the liquid yield trapping conditions of 400 °C and 2000 bars. Furthermore, the minimum trapping conditions for the type 1 complex CO_2 aqueous inclusions (nos. 13 and 33 from greisen quartz; sample P115) are considered to be 280 °C and 1000 bars, for the type 3 aqueous inclusion no. 9 (P34) estimated *P–T* conditions are 300 °C and 100 bars.

In conclusion it may be stated that during the formation of the intragranitic quartz vein and greisen quartz, the evolution of the fluids was similar, and occurred in three main stages:

Stage I. This is characterized by the trapping of complex CO_2 fluids (CO_2–N_2–CH_4–H_2S) with densities between 0.25 and 0.75 g/cm^3, and complex CO_2 aqueous fluids (H_2O–NaCl–CO_2–N_2–CH_4–H_2S) with salinities <8.5 wt.% eq. NaCl, densities from 0.5 and 0.7 g/cm^3, bulk homogenization into the gaseous state at temperatures and pressures below 700 °C and 3250 bars, respectively. Subsequently, the trapping of higher density complex CO_2 aqueous inclusions which homogenize into the liquid state occurred at temperatures and pressures below 400 °C and 2000 bars, respectively. At this stage, the density of the aqueous solutions increases, and the concentration of CO_2–CH_4–N_2–H_2S decreases as the temperature drops. For the Penouta Mine, a spatial and temporal relationship between greisenization and tin mineralization has been observed.

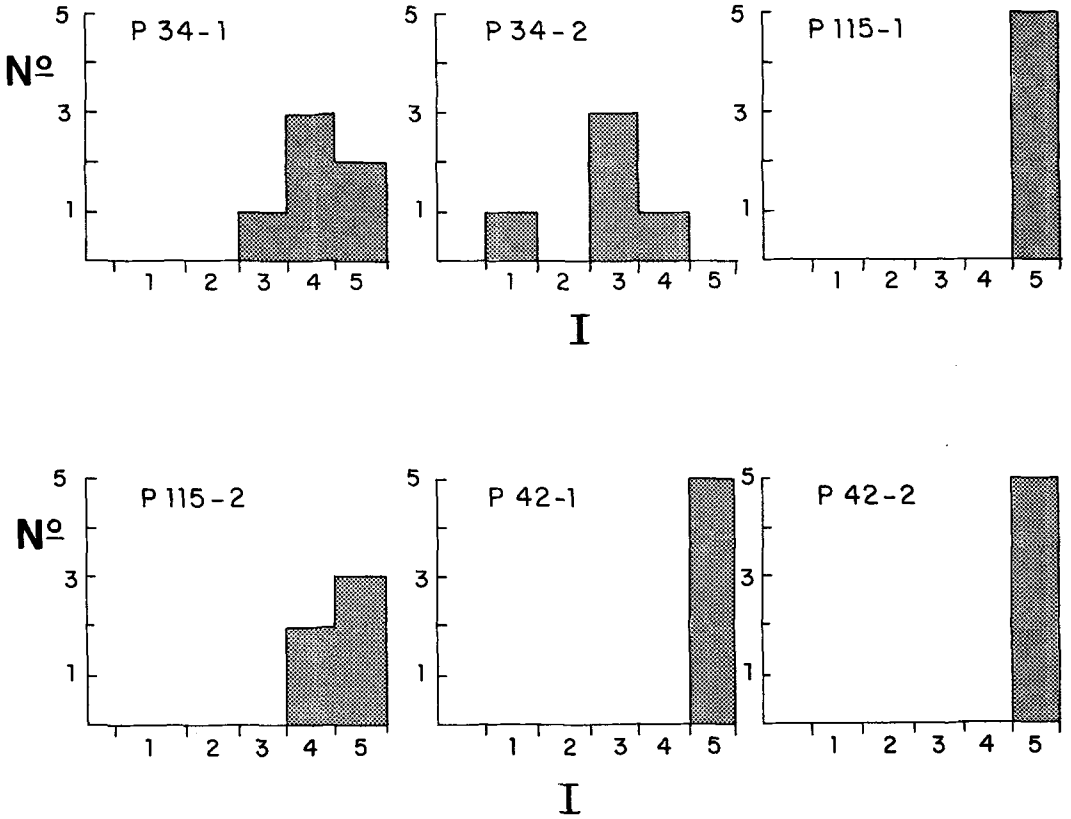

FIG. 5. Diagrams showing the results of crushing-test analyses. 1, Edge of vein and 2, core of vein. No = number of crushing-test analyses; I, liberated gas intensity, using the classification of Leroy, 1978.

Given the mineral paragenesis of the samples chosen for the study and the apparent contemporaneity of the type 1 and 2 inclusions, this implies that the inclusions are contemporaneous with greisenization. However, since different solutions are present during the early stage of mineraliz-

TABLE 3. Chemical compositions obtained by Raman microprobe spectrometry. Inclusions numbered as in Table 2 and Fig. 6. Analysts: C. Kostolanyi and J. Dubessy (C.R.E.G.U., Nancy, France). *Zi* = mole fraction of gas species *i* in the non-aqueous fluid phase, expressed in terms of mol %; *Xi* = mole fraction of species *i* in the inclusion, in mol %; d = bulk density of the inclusion in g/cm^3.

		RAMAN SPECTROSCOPY										
		MOLE FRACTION				BULK COMPOSITION AND DENSITY						
Nº F.I.	Type	Z_{CO_2}	Z_{N_2}	Z_{CH_4}	Z_{H_2S}	X_{H_2O}	X_{NaCl}	X_{CO_2}	X_{N_2}	X_{CH_4}	X_{H_2S}	d
2	1	96.41	2.60	0.99	--	94.84	0.59	4.52	0.04	0.02	--	0.90
41	1	97.37	1.69	0.94	--	92.73	0.58	6.55	0.08	0.04	--	0.68
42	1	98.24	1.15	0.47	0.15	83.96	0.80	14.97	0.17	0.06	--	0.85
13	1	94.90	2.75	2.35	--	90.52	0.86	8.29	0.16	0.14	--	0.71
33	1	95.39	2.32	2.28	--	92.74	0.58	6.52	0.09	0.09	--	0.78
19	2	96.94	2.37	0.47	0.23	--	--	96.94	2.37	0.47	0.23	0.76
9	3	--	--	--	--	98.87	1.13	--	--	--	--	0.84

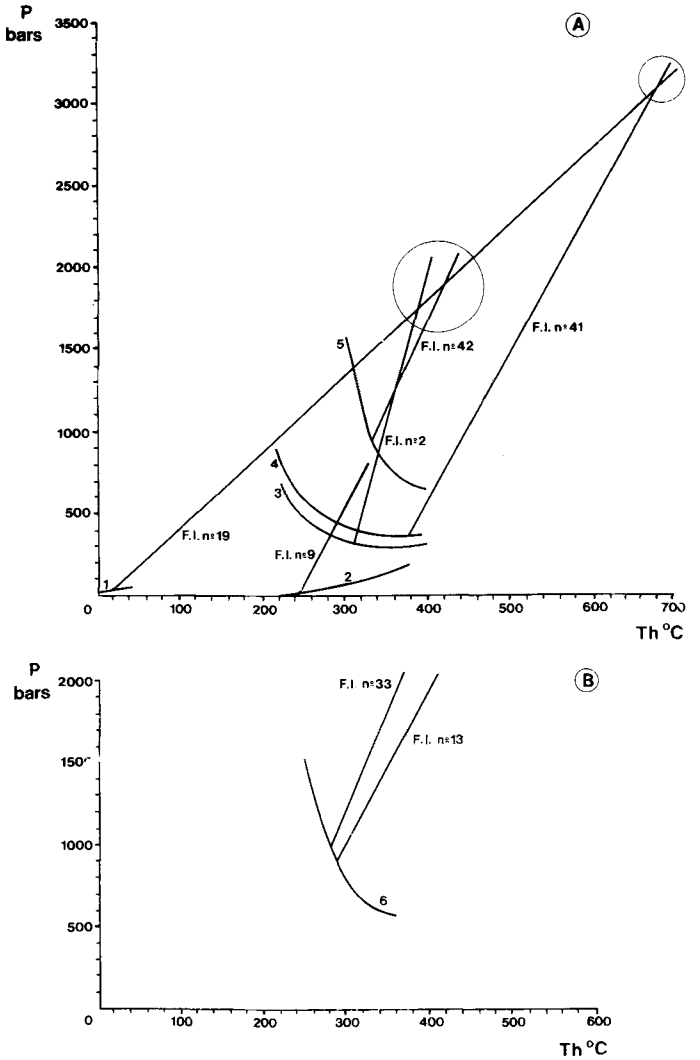

FIG. 6. Pressure–temperature diagram. Equilibrium curves and isochores corresponding to the inclusions in samples P34 and P115 for Raman spectroscopic analyses (Tables 2 and 3). 1, CO_2; 2, H_2O; 3, 5.5% mol CO_2 and 2.5% eq. NaCl; 4, 6.5% mol CO_2 and 2% eq. NaCl; 5, 15% mol CO_2 and 2.5% eq. NaCl; 6, 7.5% mol CO_2 and 2.5% eq. NaCl. The upper circle shows the intersection between type 1 inclusion which homogenizes into the gaseous state and type 2 inclusion. The lower circle shows the intersection between type 1 inclusions which homogenize into the liquid state and type 2 inclusion.

ation, it cannot be determined precisely which fluids are responsible for the alteration, and which relate to the transport and precipitation of cassiterite. Despite this uncertainty, if the results obtained for Penouta are compared with those of other tin deposits, the following conclusions may be deduced:

1. Estimated trapping temperatures for the first stage 250–700 °C are consistent with the thermal conditions (200–650 °C) calculated by various authors for granite greisenization and associated tin mineralizations (Scherba, 1970; Naumov and Ivanova, 1971; Tugarivov and Naumov, 1972; Charoy, 1979; Ramboz, 1980; Mangas, 1981 and 1987; Thomas, 1982; Roedder, 1984; Dubessy *et al.*, 1987; Cathelineau *et al.*, 1988; Durisova, 1988).

2. Estimated trapping pressures (300–3250 bars) are typical for orebodies associated with granitic intrusions, where repeated fractur-

ing of the granite permits changes in pressure, composition and temperature for each phase of fracture opening and sealing (Charoy, 1979; Ramboz, 1980; Thomas, 1982).

3. The fluids are of primarily low salinity, carbonated sodium chloride solutions (<8.5 wt.% eq. NaCl). Such low salinities are characteristic of the fluids associated with greisenization (Beus, 1967; Scherba, 1970; Charoy, 1979; Durisova, 1978; Ramboz, 1980; Mangas, 1981 and 1987; Thomas, 1982; Roedder, 1984 and Dubessy *et al.*, 1987). Likewise, the presence of CO_2 in the mineralizing solutions is common although the absolute concentration may be variable (Goncharov and Vorontsova, 1976; Ramboz, 1980; Mangas, 1981 and 1987; Roedder, 1984; Dubessy *et al.*, 1987).

Thus, the residual tin that did not crystallize with the Penouta apogranite, together with that which was released during alteration, could be transported: (*a*) in the form of complexes of the type Na{K Sn $m(CO_3)n$ (Cl,OH)p} and Na K {Sn(Cl, OH)n} (Scherba, 1970); (*b*) Cl^- and OH^- complexes in aqueous solutions at temperature around 350 °C (Jackson and Helgeson, 1985); and (*c*) as chloride complexes between 500 and 600 °C at low oxidation states (Dubessy *et al.*, 1987). The solubility of cassiterite in NaCl fluids increases with increasing temperature, oxygen fugacity and salinity (Eadington, 1983; Eugster and Wilson, 1985; Jackson and Helgeson, 1985). Hence the precipitation of cassiterite will take place as a result of sharp decreases in pressure, temperature, oxygen fugacity and salinity, or as indicated by Volosov *et al.* (1981), Halley *et al.* (1984), Jackson and Helgeson (1985), and Sushchevskaya *et al.* (1985), due to pH increases at temperatures between 300 and 500 °C.

Stage II. The second stage is characterized by low salinity, aqueous inclusions (<7 wt.% eq. NaCl), trapped at temperatures less than 300 °C and pressures below 100 bars. Also present during Stage II are very low salinity fluids, with values <4 wt.% eq. NaCl, at homogenization temperatures between 110 and 180 °C. These fluids are thought to be responsible for the kaolinization at Penouta. This is in general agreement with the work of Charoy (1979), Jackson *et al.* (1977) and Bristow (1977) who, having studied the kaolin deposits of SW England (United Kingdom) and Brittany (France), conclude that kaolinization was due to circulation of low salinity, aqueous fluids (2 and 3 wt.% eq. NaCl) at temperatures below 200 °C, pH is estimated to be 4–4.8.

Stage III. The third stage is represented by higher salinity aqueous inclusions (>13.5 wt.% eq. NaCl) with homogenization temperatures below 130 °C. These are thought to be related to the epigenetic or supergene phases of the orebody. The differences in composition and salinity for the second and third stages could be a result of mixing between magmatic fluids with formational waters. However, to confirm this hypothesis, it would be necessary to carry out isotopic studies.

The evolution and physico-chemical characteristics of the fluids of the Penouta deposit are similar to those described for the greisen and quartz veins of the Golpejas apogranite (Mangas and Arribas, 1984; Mangas, 1981, 1987). However, the pressure conditions of greisenization and precipitation of cassiterite are different. Thus, at Golpejas, pressures are estimated to be less than 900 bars. This may reflect different levels of emplacement, since at Golpejas the orebody consists of several sheets of mineralized albitic granite, while at Penouta there is a small granitic stock. These different morphologies indicates distinct emplacement depths, the Golpejas granite being intruded at a higher level that the Penouta granite.

Conclusion

The greisenization and tin mineralization at the Penouta mine was caused by essentially aqueous fluids with some volatiles (CO_2, N_2, CH_4 and H_2S). Salinities were below 8.5 wt.% eq. NaCl, densities between 0.5 and 0.8 g/cc, temperatures below 700 °C and pressures below 3250 bars. The tin was probably transported as aqueous, chloride and/or carbonate complexes. Consequently, changes in the physico-chemical conditions (i.e. temperature, pressure, density, composition and concentration) were enough to cause destabilization of the tin complexes and give rise to the precipitation of cassiterite. Thee changes occurred when the mineralizing fluids reacted with the host rocks or mixed with non-magmatic fluid.

Kaolinization of Penouta was probably generated by aqueous solutions with salinites <7 wt.% eq. NaCl, densities between 0.8 and 1 g/cm^3, homogenization temperatures between 100 and 300 °C and homogenization pressures less than 100 bars.

Acknowledgements

The work was supported by grants from the Geology Department (Salamanca), the Ministry of Universities and Research and the Polytechnical University of the Canary Islands. We thank B. Poty for access to the laboratories at C.R.E.G.U. (Nancy, France). We also

acknowledge C. Kosztolanyi for his help with the Raman analyses and J. Dubessy for providing the computer programs to calculate bulk composition, density and isochores from Raman spectroscopic data. We gratefully acknowledge A. Weisbrod, C. Leroy and J. Dubessy for their advice on all aspects of thermobarometric interpretation and the management and staff of the Penouta mine for permission to work on their property. Finally, we would like to thank Jean P. LeGrow for her translation work.

References

Angus, S., Armstrong, K. M., de Reuck, V. V., Altunin, O. G., Chapela, G. A., and Rowlinson (1976) *International thermodynamic Tables of the fluid state*. Vol. 3, Carbon dioxide: Pergamon Press. Oxford, England, 385 pp.

Arribas, A. (1979) Mineral paragenesis in the Variscan metallogeny of Spain. *Stud. Geol.*, **14**, 223–60.

Bergman, S. C. (1982) *Petrogenetic aspects of the alkaline basaltic lavas and included megacrystals and nodules from the lunar crater volcanic field, Nevada, USA*. Ph.D. dissertation Princeton University. Princeton N.J. (unpublished).

Beus, A. A. (1967) Geochemical analysis of the phenomena of high-temperature postmagmatic metasomatism and ore formation in granitoids. In *Chemistry of the Earth's crust* (Vinogradov, ed.) Israel program Sci. Transl. Jerusalem, vol. 1, 186–204.

Bodnar, R. J. (1983) A method of calculating fluid-inclusion volumes based on vapor bubble diameters and *P–V–T–X* properties of fluid inclusions. *Econ. Geol.*, **78**, 535–42.

Bristow, C. M. (1977) A review of the evidence for the origin of the kaolin deposits in Southwest England. *Proc. 8th Intern. Kaol. Symp. Meet. on alunite*, 1–19.

Cathelineau, M., Marignac, C., Dubessy, J., Poty, B., Weisbrod, A., Ramboz, C., and Leroy, J. (1988) Fluids in granitic environment. *Rend. Soc. Itl. Mineral. Petrol.*, **43–2**, 263–74.

Capote, R. (1983) Formaciones porfiroides. *Libro Jubilar de J. M. Rios. Geologia de España. Ed. Inst. Geol. Min. de España, Madrid*, 84–91.

Charoy, B. (1979) Définition et importance des phénomènes deutériques et des fluides associés dans les granites. Conséquences métallogenéniques. *Sci. de la Terre*, Nancy, Francia, Mém. no. 37, 364 pp.

Collins, P. L. F. (1979) Gas hydrates in CO_2-bearing fluid inclusions and the use of freezing data for estimation of salinity. *Econ. Geol.*, **74**, 1435–44.

Crawford, M. L., Filer, J., and Wood, C. (1979) Saline fluid inclusions associated with retrograde metamorphism. *Bull. Min.*, **102**, 562–8.

Dhamelincourt, P., Beny, J. M., Dubessy, J., and Poty, B. (1979) Analyse d'inclusions fluides à la microsonde MOLE à effet Raman. *Bull. Soc. Franc. Min. Crist.*, **102**, 600–10.

Dubessy, J., Ramboz, C., Nguyen-Trung, C., Cathelineau, M., Charoy, B., Cuney, M., Leroy, J., Poty, B., and Weisbrod, A. (1987) Physical and chemical controls (f_{O_2}, *T*, pH) of the opposite behaviour of U and Sn–W as exemplified by hydrothermal deposits in France and Great Britain, and solubility data. *Bull. Minéral.*, **110**, 261–81.

Durisova, J. (1978) Geothermometry in the minerals from the tin-ore deposit (G.D.R.) by means of gas–liquid inclusions. *Z. Angew. Geol. D.D.R.*, **20**, 352–63.

—— (1988) Diversity of fluids in the formation of ore assemblages in the Bohemian Massif (Czechoslovakia). *Bull. Minéral.*, **111**, 477–92.

Eadington, P. J. (1983) A fluid inclusion investigation of ore formation in a tin-mineralized granite, New England, New South Wales. *Econ. Geol.*, **78**, 1204–21.

Eugster, H. P. and Wilson, G. A. (1985) Transport and deposition of ore-forming elements in hydrothermal systems associated with granite. In *H.H.P. granites, hydrothermal circulation and ore genesis*, Inst. Mining Metall. 87–98.

Fisher, J. R. (1976) The volumetric properties of H_2O—a graphical portrayal. *J. Res. U.S. Geol. Surv.*, **4**, 189–93.

Gehrig, M. (1980) *Phasengleichgewichte und PVT daten ternärer mischungen aus wasser, kohlendioxid und natriumchlorid bis 3 Kbar und 550 °C*. Thesis, Institute of Physical Chemistry, University of Karlsruhe, Karlsruhe (unpublished).

Goncharov, V. I. and Voronstsova, L. A. (1976) Hydrothermal solution compositions for some Yakutian tin deposits. *Geoch. Inst.*, **13**, no. 5, 27–33.

Halley, S., Salomon, M., and Higgins, N. C. (1984) Pressure, temperature and source conditions for the fluids of the Aberfoile (Tasmania) tin tungsten vein system. *27 Congr. Int. Geol. (Moscow)*. Abstr., vol. IV (sect. 8–9), 55–6.

Iglesias, M. and Varca, R. (1981) *Mem. del Mapa Geol.*, no. 228, 1:50000. Serv. Public. Inst. Geol. Min. España.

Jackson, N. J., Moore, J. Mc. M., and Rankin, A. H. (1977) Fluid inclusions and mineralization at Cligga Head, Cornwall, England, *J. Geol. Soc. London*, **80**, 1365–78.

Jackson, K. J. and Helgeson, H. C. (1985) Chemical and thermodynamic constraints on the hydrothermal transport and deposition of tin: calculation of the solubility of cassiterite at high pressures and temperatures. *Geochim. Cosmochim. Acta*, **49**, 1–22.

Leroy, J. (1978) Métallogenèse des gisement d'uranium de la division de la Crouzille. (Cogema-Nord Limousin, France). *Memor. Sci. de la Terre, Nancy, France. Mém.* no. **36**, 276 pp.

Mangas, J. (1981) *Estudio microtermométrico del yacimiento de Golpejas (Salamanca)*. Tesis Licenciatura, Universidad de Salamanca, Salamanca, 103 pp. (unpublished).

—— (1987) *Estudio de las inclusiones fluidas en los yacimientos españoles de estaño asociados a granitos hercínicos*. Tesis Doctoral, Universidad de Salamanca, Salamanca, 644 pp. (unpublished).

—— and Arribas, A. (1984) Evolución y características de las fases fluidas asociadas a los filones de cuarzo del yacimiento estannifero de Golpejas (Salamanca). *I Congreso Español de Geología, Segovia*, **2**, 551–64.

Naumov, V. S. and Ivanova, G. F. (1971) The pressure and temperature conditions for formations of wolframite deposit. *Geochim. Intern.*, **8**, no. 3, 381–93.

Potter, R. W., Clinne, M. A., and Brown, D. L. (1978) Freezing point depression of aqueous sodium chloride solution. *Econ. Geol.*, **73**, 284–5.

Poty, B., Leroy, J., and Jachimowicz, L. (1976) Un nouvel appareil pour la measure des températures sous le microscope: l'installation de microthermométrie chaix-meca. *Bull. Soc. Fr. Minéral. Cristall.*, **99**, 182–6.

Ramboz, C. (1980) *Géochimie et étude des phases fluides de gisements et indices d'etain-tungstène du Sud du Massif Central (France)*. Thèse de 3éme cycle. Nancy. 278 pp. (unpublished).

—— Schanpper, D., and Dubessy, J. (1985) The P–V–T–X–f_{O_2} evolution of H_2O–CO_2–CH_4-bearing fluid in a wolframite vein: reconstruction from fluid inclusion studies. *Geochim. Cosmochim. Acta*, **49**, 205–19.

Roedder, E. (1984) Fluid inclusions. *Reviews in Mineralogy*, **12**, Mineral. Soc. Amer., Blacksburg, Va, 644 pp.

Scherba, G. N. (1970) Greisens. *Inst. Geol. Rev.*, **12**, no. 2, 114–150, and no. 3, 239–55.

Sushchevskaya, T. M., Luchitskaya, M. I., Ryzhenko, B. N., and Barsukov, V. L. (1985) Acidity of the medium during hydrothermal cassiterite formation. *Geoch. Int.*, **21**, 77–87.

Swanenberg, H. (1979) Phase equilibria in carbonic systems and their applications to freezing studies of fluid inclusions. *Contrib. Mineral. Petrol.*, **68**, 303–6.

Thomas, R. (1982) Ergebnisse der thermobarogeochemischen untersuchungen and flüssigkeitsinschlüssen in mineralen der postmagmatischen tinn-wolfram-mineralization des Erzgebirges, Freiberg, Forschungsh., Reihe C, no. C370, 85 pp.

—— Tugarinov, A. I. and Naumov, V. B. (1972) Physicochemical parameters of hydrothermal mineral formation. *Geoch. Int.*, **9**, no. 2, 161–7.

Volosov, A. G., Borisov, M. V., Sushchevskaya, T. M., and Knyazeva, S. N. (1981) Deposition of cassiterite during formation of hydrothermal tin ore deposits according to the results of physico-chemical modelling. *Geochem. Int.*, **18**, 49–66.

[*Manuscript received 6 September 1989; revised 1 August 1990*]